THE APPLICATION OF OPTIMAL WAVELETS IN SEISMIC INVERSION

SUDHIR JAIN* AND A. EASTON WREN**

ABSTRACT

The current emphasis in seismic stratigraphy has focussed on velocity inversion and the generation of the pseudo-acoustic log from the seismic trace. There are several published methods on wavelet extraction which invariably make assumptions about the wavelet, in terms of the phase spectrum, as well as assumptions about the reflectivity.

The SONISEIS method will provide the basic wavelet using a statistical estimation, independently of any assumptions about the wavelet. The derived wavelet is replaced in the seismic trace with a spike of appropriate amplitude and polarity. This process of wavelet extraction, followed by the derivation of the reflectivity sequence, allows the ideal pre-conditioning for seismic velocity inversion.

The significance of this approach is demonstrated in a series of synthetic and real data examples. The statistically computed wavelets allow for synthetic seismograms which consistently outmatch those with Ricker or best-estimate zero or minimum-phase wavelets.

INTRODUCTION

Although the computation of velocities from reflection seismic data has been a standard practice for many years (Green 1938, Dix 1955), inversion of the seismic trace, or the reduction of a seismic trace to a sampled log of interval velocities in the transmitting medium, was first introduced in 1970 at a meeting of the European Association of Exploration Geophysicists in Edinburgh (Delas et al 1970). This approach was subsequently discussed by Lavergne (1974) and Lindseth and Street (1974) and several companies have introduced their version of this technique over the last year.

Derivation of interval velocities from seismic reflection amplitudes can be viewed as the next evolutionary stage to 'bright spot' analysis. The development of this processing technology has historically been hindered by several factors; lack of true amplitude (for true reflectivity), severe filtering in the field resulting in limited bandwidth and possibly a lack of appreciation of the seismic implications in exploring for stratigraphic traps.

In exploration for structural traps, the relative amplitude of reflections and the interval velocities of various layers are of little significance. The large scale stratigraphic variations can often be deduced from velocities computed for normal moveout corrections. However, the exploration for subtle stratigraphic traps focussed interest on bright spots in the early seventies and drew attention to the relationship between reflection amplitude and the velocity of the material across the interface. It was quickly realized that the resolution of normal seismic reflection events spanning 30-60 msecs. on a trace was inadequate to define layers even up to 100 feet thick. This desire for greater resolution spurred heightened interest in detailed inversion techniques.

The integration of a normally processed seismic trace, even after phase compensation, is not enough

Presented at the 47th Annual Meeting, September 14th, 1977 in Calgary. Publication authorized by the Editor, Geophysics.

* Commonwealth Geophysical Development Company Ltd., Calgary, Alberta

**PanCanadian Petroleum Limited, Calgary, Alberta

to resolve thin reservoirs of current exploration interest. It is necessary to derive the seismic wavelet and replace it with a spike of appropriate magnitude and polarity. The resulting reflectivity series will have considerably better resolution than the seismic trace and the velocities computed from this series will be more accurate than those computed directly from the trace.

In this paper, we describe a method of deriving an optimum wavelet from the seismic trace and its application to compute the reflectivity series and the interval velocity distribution. The system of programs to implement this method is called SONISEIS.

State of the Art

The seismic trace represents the reflectivity series convolved with the seismic wavelet and the impulse response of the recording system which includes source and receiver arrays, geophones, recording instruments and aliasing filters. In the general case of an inelastic transmission medium, this seismic wavelet suffers frequency distortion as it propagates. However, in practice, it can be assumed that over restricted travel time zones of the duration of .5, 1.0 or even 2.0 seconds of two-way time, it is fairly uniform and experience has shown this assumption to be justified. Deconvolution applied in early processing stages no doubt assists in stabilizing the wavelet — indeed this is the primary function of deconvolution.

The problem of inverting the trace is basically that of determining the wavelet, or a close approximation of it. Once the wavelet is known, it can be replaced by a spike of appropriate amplitude at the onset of the wavelet using established techniques (Rice 1962). The result of this substitution is a close approximation to the reflectivity indices encountered by the wavelet.

There are several methods of determining the wavelet:

1) Assume that the spectrum of the reflectivity series is white. Therefore, the power spectrum of the trace represents the spectrum of the wavelet. The next assumption is that the wavelet is minimum phase (Robinson and Treitel,

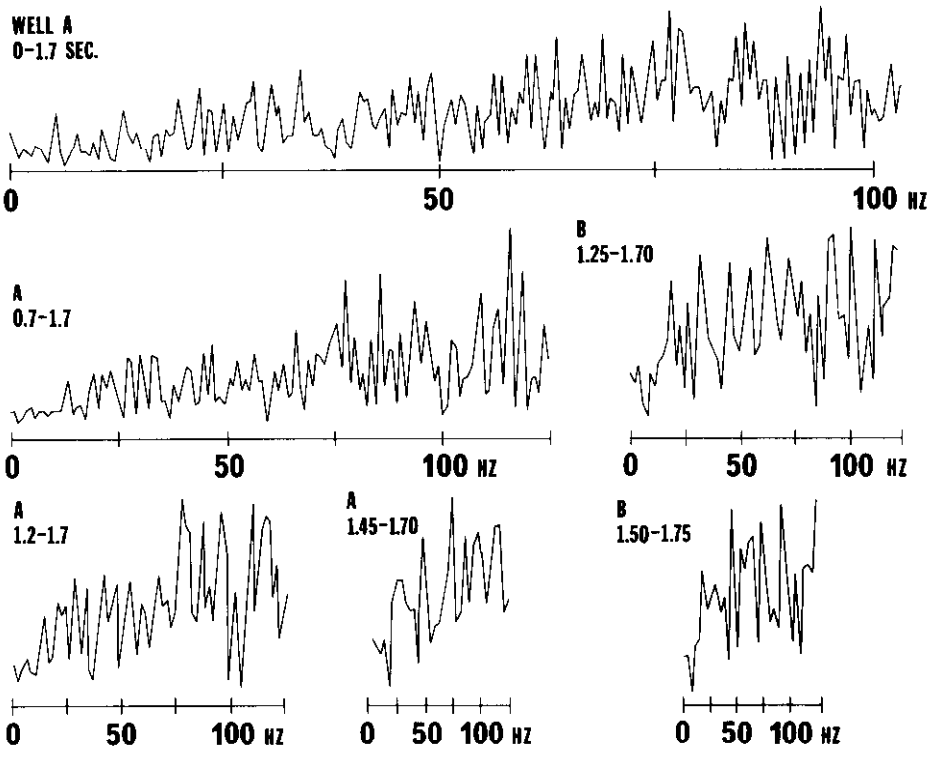

Fig. 1. Power spectra over various windows of the reflectivity series computed from two wells in Alberta.

1976). White and O'Brien (1974) discussed this approach from a practical viewpoint. Computing this phase and subtracting it from the actual phase component of the trace gives the reflectivity series. The basic problem with this approach is that the spectrum of the reflectivity series may not be white. Figure 1 shows the power spectra over the reflectivity series computed from the velocities logged in two wells in Alberta. Even for a long window, the spectrum can hardly be regarded white and obviously an approach assuming it to be so will be erroneous.

A second objection to this approach is that the wavelet may not be minimum phase as it would be in perfect transmission medium. If one considers the weathering layer, miscellaneous instrument responses, shot hole response, source and receiver arrays, the 'ideal' wavelet is likely to be a rare occurrence.

2) Assume that the reflectivity series is minimum phase and compute the phase of the wavelet by homomorphic deconvolution (Buttkus 1975, Stoffa et al 1974). The wavelet and the reflectivity series can be separately identified in the cepstrum of the trace and the transfer back into the time domain of the separated parts of cepstrum provides both the wavelet and the reflectivity series.

   This approach has promise although problems are encountered in separating reflectivity series from the wavelet in the cepstrum and in making sure that the reflectivity series is minimum phase. In addition, the process is very sensitive to noise.

3) The wavelet can be taken directly from the trace provided one or more isolated events (eg: water bottom) can be identified (Delas et al, 1970). In practice, there are no isolated reflectivity indices in the subsurface and there are no 'clean' events. This approach is dangerous because the combination of reflectivities which influence the wavelet will be transferred to all other data, thus causing errors.

4) Burg's technique (Claerbout 1976) and direct deconvolution methods make the assumption of minimum phase and again are fairly successful when this assumption is valid.

Determination of the Optimum Wavelet

The wavelet is described as the composite of all the external influences which transform the source spike into a long bandlimited wavelet. These factors include source and receiver environment, unconsolidated near surface material, instrument response and frequency absorption in the transmission medium of imperfect elasticity. At least some of the effects due to the last factor are compensated by deconvolution and experience shows that the wavelet in a processed true amplitude section is fairly uniform. The computation of this composite wavelet from the data provides a close approximation of the reflectivity series following the technique described by Rice (1962).

The problem of computing the wavelet from the trace can be better understood in the frequency domain. The trace, being a convolution of the reflectivity series R and the wavelet W, is represented by:

$$S(f).e^{i\phi_S(f)} = R(f).W(f).e^{i(\phi_R(f)+\phi_W(f))}$$

where ϕ represents phase.

To isolate W(f) some assumption has to be made about R(f), the normal assumption being R = 1 (reflectivity index series is white). Similarly to determine $\phi_R(f)$ from $\phi_S(f)$ one has to make some assumption about $\phi_W(f)$. Normally, one (ϕ_R or ϕ_W) is assumed minimum phase.

In this inversion approach, R(f) is assumed to be approximately white and W(f) is a smoothed version of S(f). The type and degree of smoothing necessary for the optimum computation was determined after extensive experimentation and has been confirmed with real data cases over the last twelve months. The phase assumption is optional. The user can select minimum phase, zero phase or computed phase wavelets. The first two types of wavelets are computed in the standard manner from the amplitude spectrum W(f). To compute the phase in the last option (computed phase), the phase spectrum of the trace is smoothed and the smoothed phase spectrum adjusted automatically. Again, the degree of smoothing and the adjustment were determined from numerous experiments and have been repeatedly confirmed in practice.

Application of the Inversion Process

The data to be 'inverted' do not require any *special processing other than true amplitude* preservation and minimum of bandlimiting filters. Excessive band limiting must be avoided, but the *inclusion of frequencies with poor signal/noise ratio* causes errors which outweigh the benefits of better resolution. Any time variant scaling, deconvolution *or filtering is avoided. When the signal/noise ratio* is poor, the data may be processed through a multi-channel coherency enhancement process. In *structurally complex areas, migration is desirable.*

The reflectivity series computed by trace inversion is proportional to the actual reflectivity series. The constant of proportionality is computed either from a nearby well or by visual inspection. Also, the velocity variations of very low frequency are not represented in the computed reflectivity series because most data undergo low-cut filtering in some form. These velocity variations are computed either from normal moveout velocities or from velocities logged in neighbouring wells. Densities are computed using empirical velocity-density relationships given by Gardner et al (1974). The standard equation relating reflectivity series to acoustic impedence (Dobrin 1977) is used to compute successively the velocities immediately below the layer represented by each sample.

Synthetic Example 1 — Known and Computed Wavelets

Figure 2 shows a synthetic trace generated by convolving a Ricker wavelet with a reflectivity sequence designed to test the accuracy of the process. In the first instance, the wavelet, the reflectivity series and the velocities are computed by the inversion process. In the second instance, the known wavelet is used to compute the reflectivities and the velocities. Figure 3 shows the computed wavelet and the input Ricker wavelet. Undoubtedly, the process has successfully recovered the wavelet. With the known wavelet, the recovery of the reflectivity series and velocity distribution is almost perfect. When the wavelet is computed, small differences between actual and computed wavelets are not critical for reflectivity estimate and layers as thin as 4 msec. can be identified but with some reduction in amplitude.

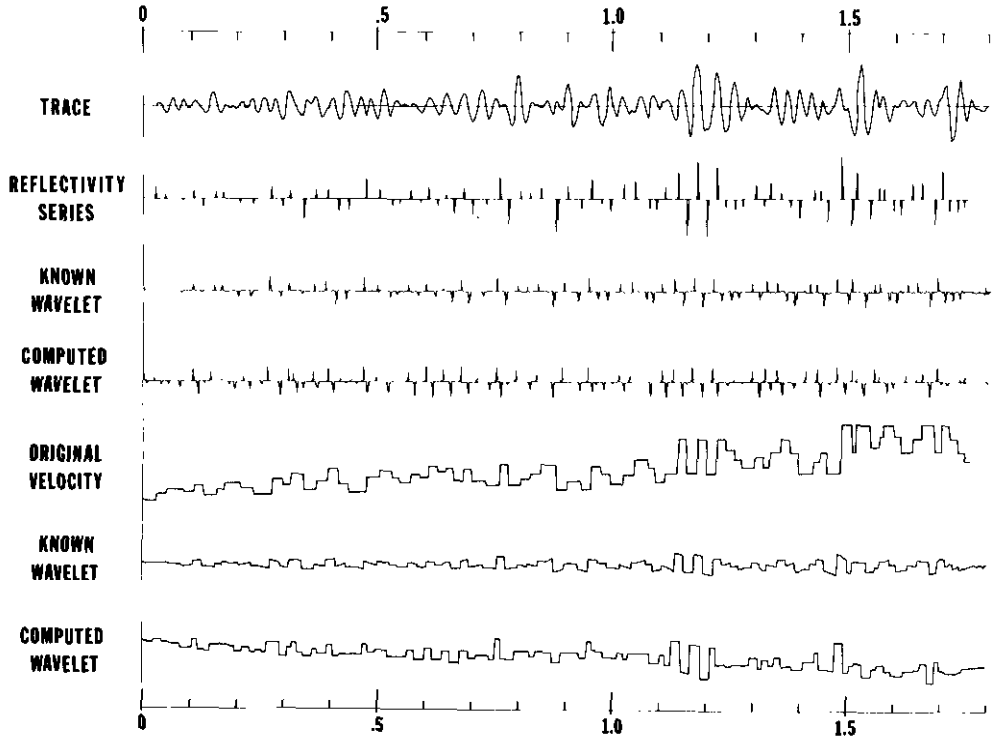

Fig. 2. Comparison of the results of the inversion process when the wavelet is known and when it is computed.

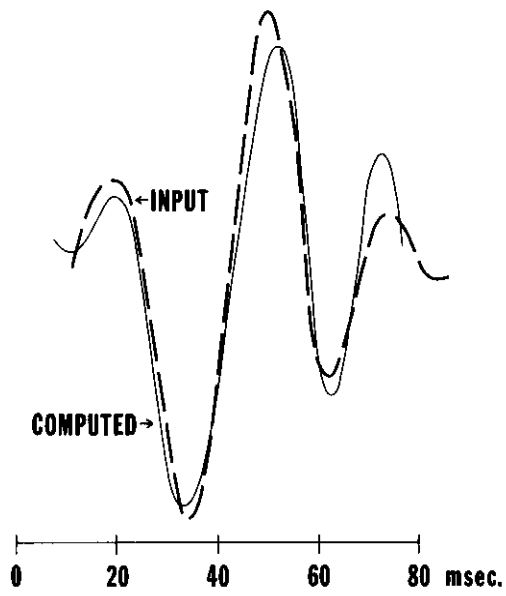

Fig. 3. The input wavelet and the computed wavelet for the synthetic model shown in Figure 2.

Synthetic Example 2 — Well From Alberta

The integrated velocities logged in a well in Alberta were used to generate a synthetic seismogram. A Ricker wavelet of 38.4 Hz was used in the convolution. Figure 4 shows the actual velocities from the well, those computed by inversion of the seismogram using the known wavelet, the minimum phase wavelet and the computed phase wavelet. The corresponding velocities are shown in the same order in Figure 5 after applying a five point (2 msec. interval) constant smoothing operator.

The figures illustrate excellent recovery of the velocity variations greater than 8 msec. peak to peak by each wavelet. The loss of resolution for layers thinner than 8-10 msecs. is attributed to the low frequency characteristics of the wavelet.

Even though the resolution of very thin layers is not possible, the unfiltered velocity plots in Figure 4 are preferable because they indicate the locations and thicknesses of identified layers exactly.

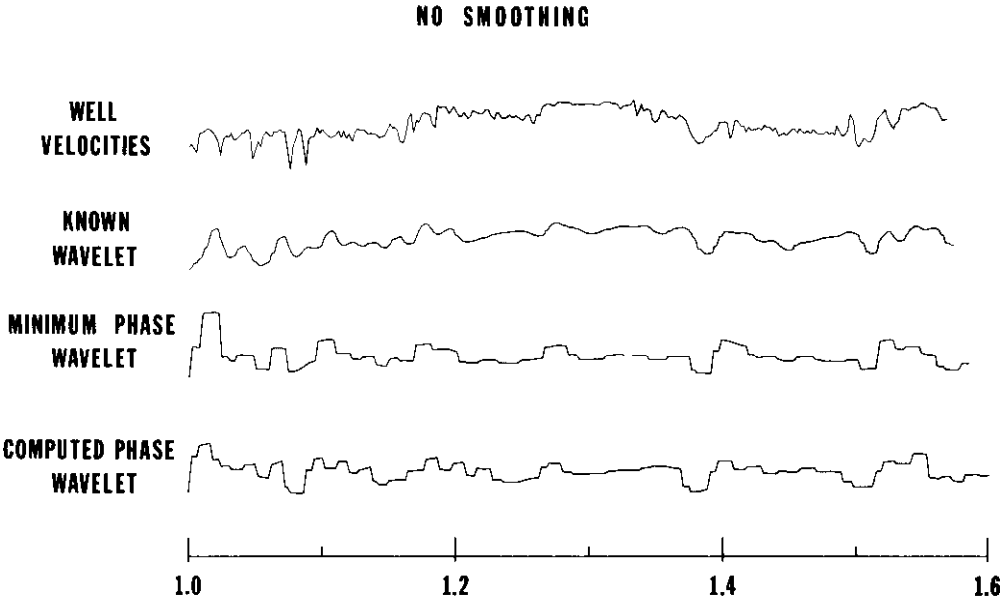

Fig. 4. The velocities computed by the inversion process from the synthetic seismogram compared to the actual velocities in the well.

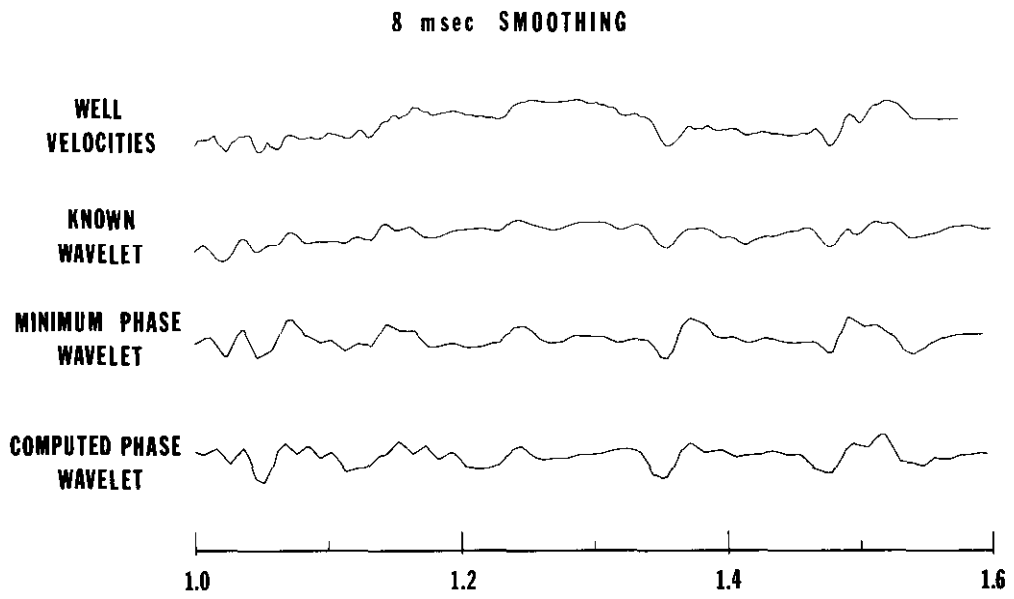

Fig. 5. The velocities computed by the inversion process from the synthetic seismogram compared to the actual velocities in the well after 8 msec. smoothing operator.

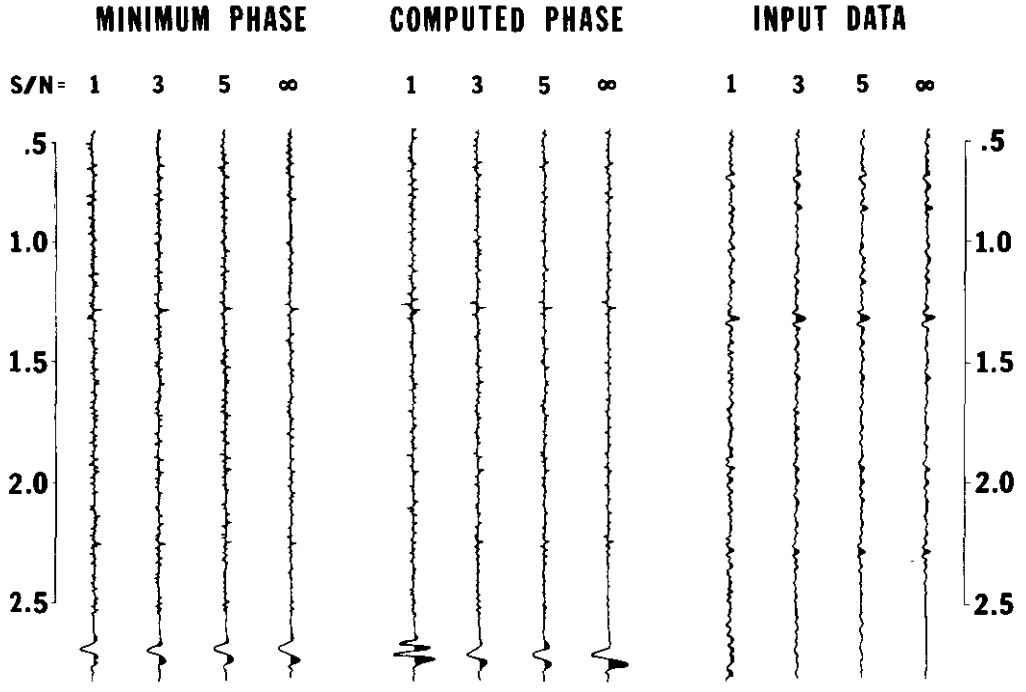

Fig. 6. The synthetic trace and computed reflectivities for various signal to noise ratios. The determined wavelets are shown at the end of the reflectivity series.

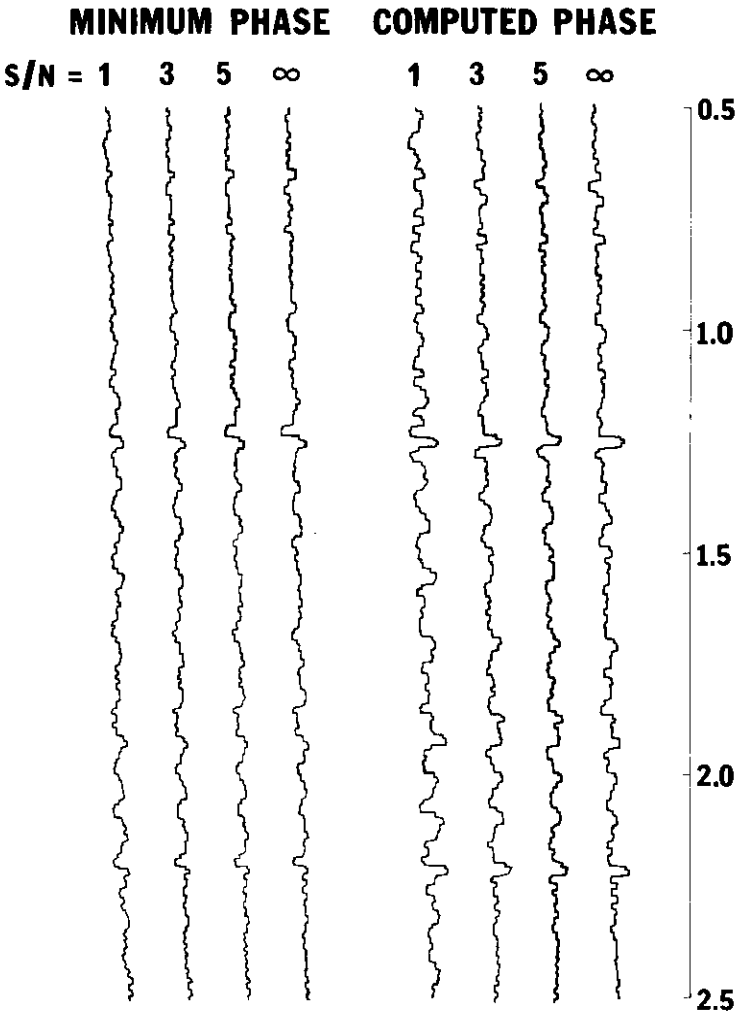

Fig. 7. The computed interval velocities from reflectivities shown in Figure 6.

The Effect of Random Noise on Inversion

The above examples demonstrate that a good approximation to the wavelet can be computed from synthetic noise free data and the reflectivity index can be recovered with reasonable accuracy. Figures 6 and 7 demonstrate the effect of random noise on the process.

Figure 6 shows a noise free synthetic trace on the extreme right. The three adjacent traces were generated by adding random noise to the trace. The random series was filtered 0/10 50/70 Hz and the filtered noise was scaled to the desired ratio in relation to the total energy of the trace.

The two sets of reflectivity series computed from these traces are also shown. One set was computed assuming the wavelet to be minimum phase and the other set by computing the phase of the wavelet. The differences in the computed wavelets are very minor except when signal to noise ratio (S/N) is 1/1. This indicates that the original wavelet was perhaps minimum phase or very nearly so. Consequently, the two sets of reflectivity series are also very similar for S/N of 3/1 or better. When S/N is 1/1, the stronger reflectivities in both series correlate with the noise free reflectivity series but the smaller amplitude spikes are lost in the noise. The general similarity in the two series when S/N rate is 1/1 suggests that the differences

in wavelets are caused by the random noise and the extraction of these wavelets tends to compensate, to some extent, the effects of random noise.

Figure 7 shows the interval velocities obtained from the two sets of reflectivity series. Again, the velocities match reasonably for data with signal/noise ratio of 3/1 or better. When the S/N is 1/1, the reflectivity spikes caused by the random noise are detrimental to the velocity computations and the velocity curves show many important differences.

It appears that the inversion process is accurate when S/N is 3/1, but the ratio of 1/1 is detrimental to the inversion process. The S/N ratio of 2/1 is perhaps the transition point from satisfactory to poor inversion.

In general the experience with synthetic and real data has shown that when data has a signal/noise ratio of approximately 2:1 or less, the minimum phase wavelet is less inaccurate than the computed phase wavelet. Similarly, for trace lengths up to 250 msecs., minimum phase wavelets are more reliable. Under such circumstances, the stability of both wavelet types is enhanced by averaging over a number of traces.

Extracted Wavelet and Synthetic Seismogram

The standard synthetic seismogram is constructed from the reflectivity series (computed from the integrated velocity in the well) by convolving these with a specified wavelet. In Canada, the Ricker wavelet of main frequency 38.4 Hz is often used. In many cases, this synthetic seismogram matches the seismic sections in the area satisfactorily. However, in some cases the correlation is poor and suspicion is aroused about the quality of the seismic data or the sonic log.

Figure 8 shows a representative processed trace and six synthetic seismograms. Five of these seismograms were computed with arbitrary wavelets (including the Ricker wavelet described above) and match the trace unsatisfactorily. Some of the similarities lead to miscorrelations of other depths. The sixth seismogram uses the wavelet computed from the seismic section. This matches the data satisfactorily in spite of the lack of check shot corrections and the deviation of the well.

The good fit between actual data and synthetic seismograms computed from the derived wavelet enhances confidence in the seismic data as well as the inversion process.

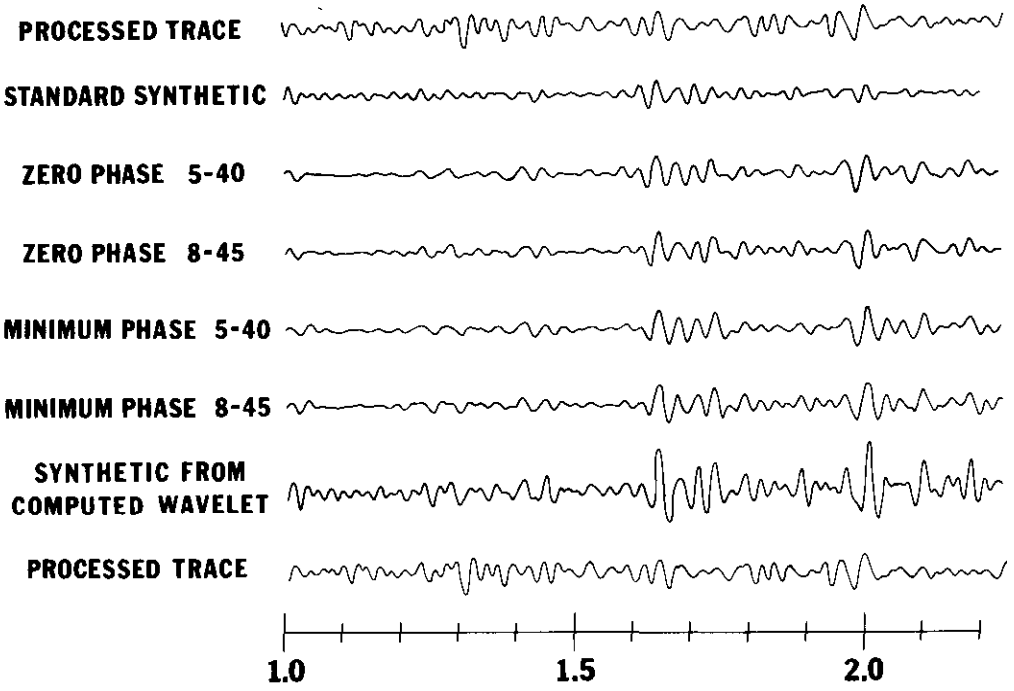

Fig. 8. Comparison of synthetic seismograms to a processed trace located at the well.

Real Data Cases

The objective of this part of the paper is to demonstrate the practical benefit of seismic inversion after optimal wavelet estimation and removal. This involves two real data examples, one land and one marine.

Example 1

The first example is from Southern Alberta. Figure 9 shows the geological environment typical of the Cretaceous in this area. The section shows a series of producing wells and dry holes — the production being from the Glauconite channel sand and bar sand reservoirs, with up to 30% porosity and net pay reaching a maximum of 65 feet. One could be optimistic that such a thick and highly porous reservoir would have a diagnostic seismic signature, but the character changes associated with the variation from porous to tight Glauconite are not obvious on the section (Figure 10). We see a subtle character change which involves a trough of lower frequency corresponding to the pay and a tightening up in frequency where the porosity is zero. Without the well control, such subtleties would be overlooked.

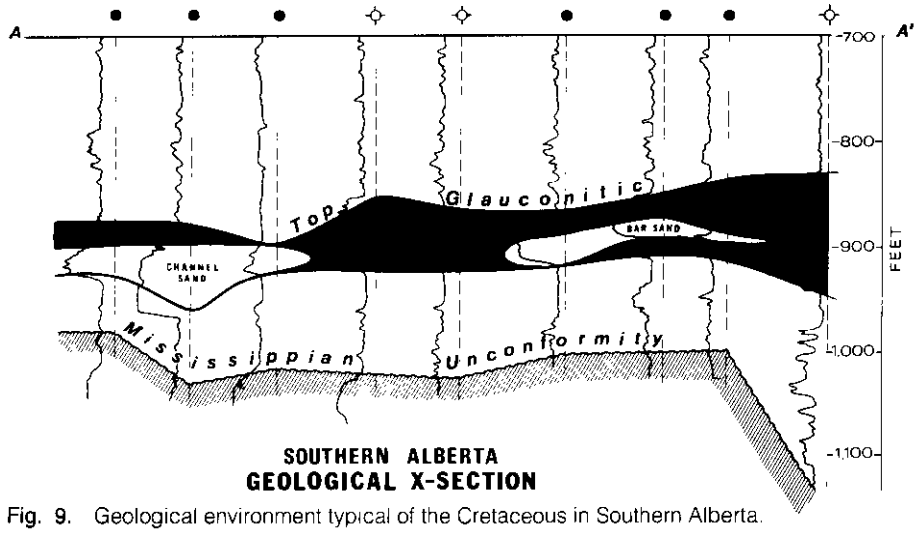

Fig. 9. Geological environment typical of the Cretaceous in Southern Alberta.

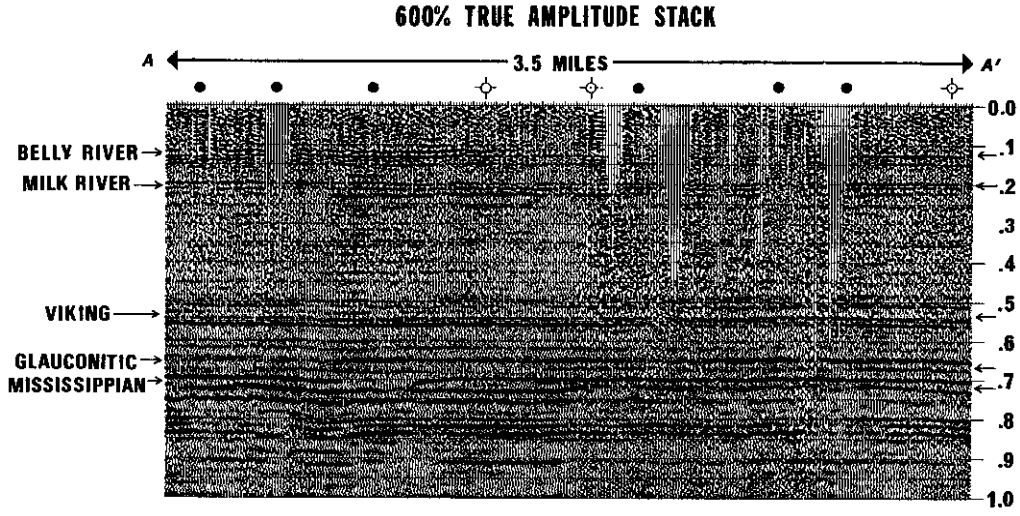

Fig. 10. Seismic reflection records covering the profile in Figure 9.

The seismic section is an early attempt at high resolution (or extended frequency) acquisition and processing. It is 600%, recorded with a DFS-IV at 1 msec. sample interval, L-1-14 Hz seismometers, 110 foot group interval, charge of 1¼ lbs. at 60 foot depth and a recording filter of 8-248 Hz. It has been processed at 1 msec. in true amplitude and has a spiking deconvolution before stack. Even with such relatively sophisticated acquisition and processing, the resolution of the pay zone is not obvious. However, by most conventional standards, this is good quality data.

Figure 11 includes a series of traces after the inversion process. These correspond to the wells with some additional infilling traces. The lower velocity zone associated with the Glauconite porosity is now readily apparent and we can see quite clearly the transition from the channel to the intervening zone and into the bar sand. The practical advantage of the inversion process in this example is self-evident and without it the interpretation of the standard seismic section would be questionable at best, even with the high density well control.

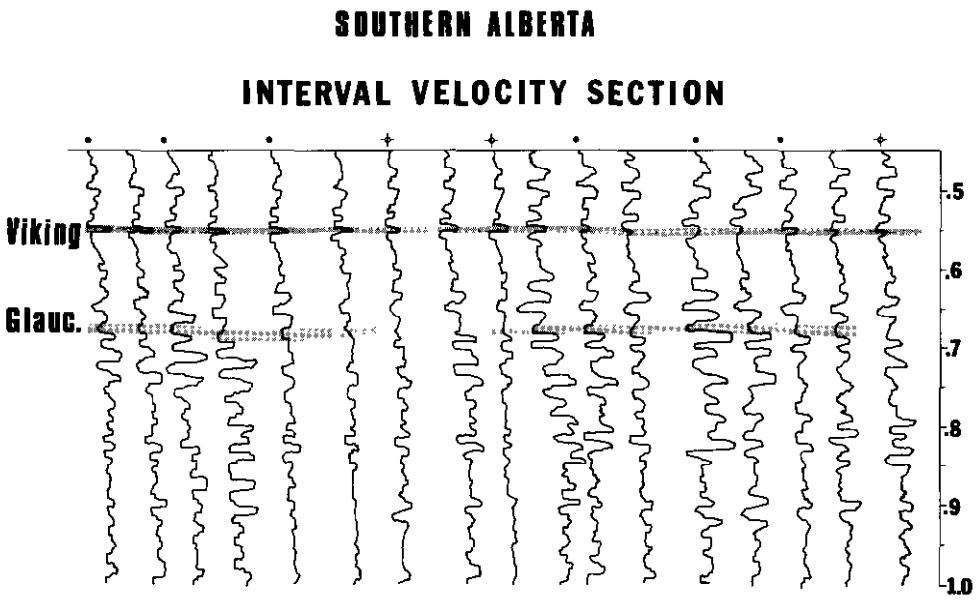

Fig. 11. Results of inversion of some of the traces shown in Figure 10.

EXAMPLE 2

The second example is from an offshore area in North America. Figure 12 depicts, from the left, three adjacent traces from the conventional true amplitude stacked section. This is from an area where geological control is sparse and there is, therefore, some question about the significance of the high amplitude event which dominates the traces. The water bottom event on these traces is misleading in that the onset does not coincide with the expected water bottom event from the known water depth. There is, therefore, some concern about the trace polarity.

The data is 2400% air gun and was recorded with a 4 msec. sample interval and an 8-62 recording filter. The water bottom multiple has been substantially suppressed by an adaptive deconvolution after stack.

The next three traces on Fig. 12 are the equivalent traces after estimation and removal of the wavelet as discussed earlier. These traces show several interesting features. We now see clear evidence of a water bottom event at the proper time and its polarity is distinctly negative. The traces are, therefore, polarity reversed. Secondly, the reflectivity series (the plotter response for 4 msec. is super-imposed on the spikes) corresponding to each geological interface is clearly defined. The prominent 'bright spot' is still evident and has been broken up into two important events. The shallower event is a peak (ie: actually a trough)

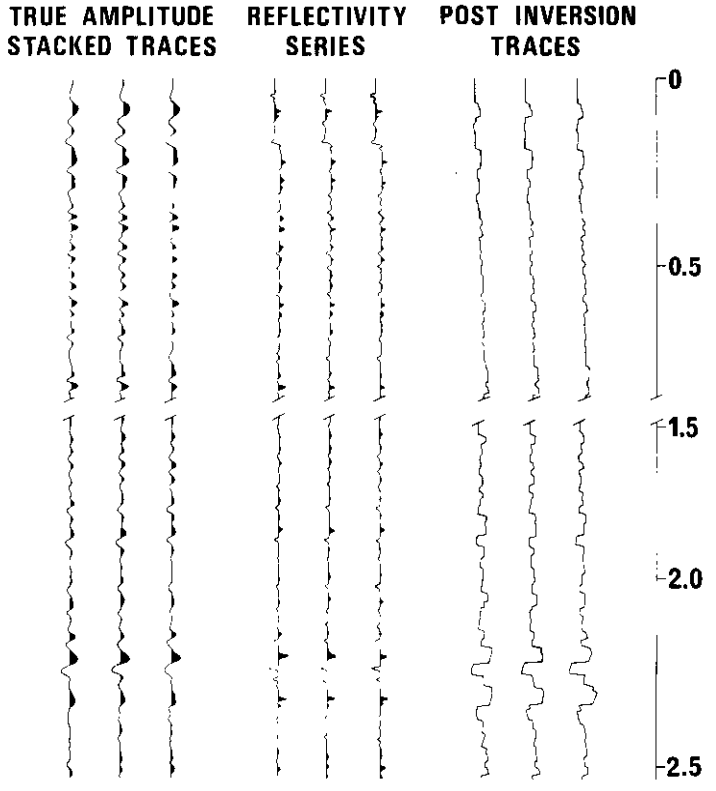

Fig. 12. Seismic traces, computed reflectivity series and interval velocities from an offshore area.

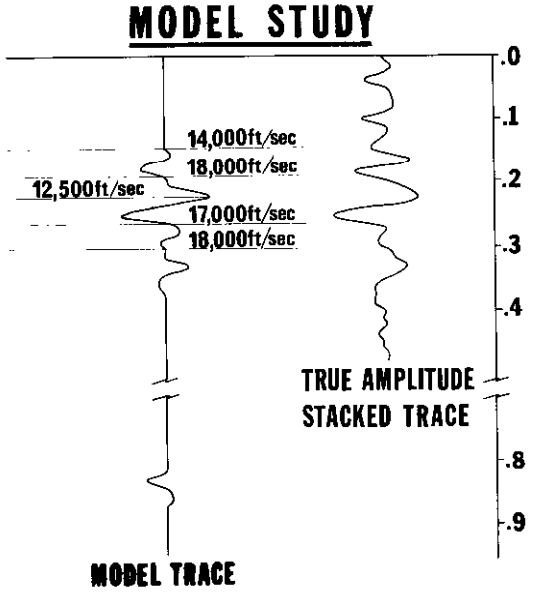

Fig. 13. The synthetic seismic response for the interpretation based on inversion shown in Figure 12 compared with the actual seismic trace.

and the two events define a low velocity zone of approximately 32 msec.

The adjacent three traces show the corresponding traces after inversion. The cross-correlation is high and the inversion is obviously very stable. There is little distortion which could be related to a poor S/N ratio. The traces were polarity reversed prior to inversion. The low velocity zone in the area of interest is now very conspicuous.

A model was designed to verify the interpretation of a low velocity layer. Figure 13 shows the synthetic seismic response using the wavelet derived prior to inversion. The wavelet is almost symmetrical and has a prominent central trough with minor lobes. Its width is 36 ms. The correlation between the synthetic trace and the equivalent trace from the true amplitude stack section is impressive.

Summary

With the current emphasis on exploration for stratigraphic traps there is a need for processing technology to define lithological signatures in seismic data which are not always evident on standard processed true amplitude seismic sections. The synthetic and real data examples have shown that the combined wavelet estimation and removal followed by the inversion process is a powerful tool which follows naturally as a corollary to 'bright spot' processing. The technique provides a high degree of thin-layer resolution even from severely bandlimited data, a reliable approach to velocity determination and a consistency of wavelet extraction which underlies the validity of the process.

We acknowledge PanCanadian Petroleum Limited and other companies for permission to use their data in this presentation.

References

Buttkus, G., 1975, Homomorphic filtering, theory and practice, Geophysical Prospecting, v. 23, p. 712-748.

Claerbout, J., 1976, Fundamentals of Geophysical Data Processing, McGraw-Hill, New York.

Delas, G., J. B. Beauchomp, G. deLombares, J. M. Fourmann, A. Postic, 1970, An example of practical velocity determinations from seismic traces. Paper presented at 32nd EAEG Meeting in Edinburgh, Scotland.

Dix, C. H., 1955, Seismic velocity from surface measurements, Geophysics, v. 20, p. 68-86.

Dobrin, M. B., 1977, Introduction to Geophysical Prospecting, McGraw-Hill, New York.

Gardner, G. H. F., L. W. Gardner, R. A. R. Gregory, 1974, Formation velocity and density — the diagnostic basics for stratigraphic traps, Geophysics, v. 39, p. 770-780.

Green, C. H., 1938, Velocity determinations by means of reflection profiles, Geophysics, v. 3, p. 295-305.

Lavergne, M., 1974, Pseudo-diagraphics de vitesse in offshore profond, Geophysical Prospecting, v. 23, p. 695-711. Also presented at the 36th Annual Meeting of the EAEG in Madrid, 1974.

Lindseth, R. O., A. V. Street, 1974, Velocity information and seismic traces. Paper presented at 44th Annual SEG Meeting held in Dallas, October 1974.

Rice, R. B., 1962, Inverse convolution filters, Geophysics, v. 18, p. 4-18.

Robinson, E. R., S. Treitel, 1976, Net down going energy and the resulting minimum phase property of down going waves, Geophysics, v. 41, p. 1394-1396.

Stoffa, P. L., P. Buhl, G. M. Bryan, 1974, The application of homomorphic deconvolution to shallow water marine seismology, Part I and II, Geophysics, v. 39, p. 401-426.

White, R. E. and P. N. S. O'Brien, 1974, Estimation of the primary seismic pulse, Geophysical Prospecting, v. 22, p. 627-651.